

# Charge transport and electronic properties of N-heteroquinones: quadruple weak hydrogen bonds and strong $\pi-\pi$ stacking interactions

Guochun Yang · Yanling Si · Yun Geng ·  
Fei Yu · Qingxiu Wu · Zhongmin Su

Received: 13 July 2010/Accepted: 20 October 2010/Published online: 11 November 2010  
© Springer-Verlag 2010

**Abstract** The charge transport and photophysical properties of N-heteroquinones, which can function as n-type organic semiconductors in organic field-effect transistors (OFETs) with high electron mobility, were systematically investigated using hopping model, band theory, and time-dependent density functional theory (TDDFT). The calculated absorption spectra and electron mobility are in good agreement with experimental results. To the studied compounds, subtle structural modifications can greatly reduce the reorganization energy. There are two main kinds of intermolecular interaction forces of the studied compounds in the crystal, which result from intermolecular  $\pi-\pi$  and hydrogen bonds interactions, respectively. The results of hopping model show that the electron transport properties are mainly determined by pathways containing intermolecular  $\pi-\pi$  interactions, and hole transport properties are mainly determined by pathways containing intermolecular hydrogen bonds from the standpoint of transfer integral. Moreover, electronic transfer integral value increases with the enhancement of intermolecular overlap corresponding to the overlap extent of  $\pi-\pi$  packing. Hole transfer integral value decreases with decreasing the number of hydrogen

bonds. This means that charge transport properties can be efficiently tuned by controlling the relative positions of the molecules and the number of hydrogen bonds. The analysis of band structure also supports the conclusion of hopping model.

**Keywords** 6,11-diaza-5,12-tetracenequinone · OFETs · Charge transport · Hopping model · Band theory

## 1 Introduction

The advantages of organic field-effect transistors (OFETs), such as low cost, flexibility, and large-area fabrication, have recently attracted much attention due to their electronic applications [1]. N-type organic semiconductors that accept and transport electrons are the key materials in organic thin-film transistors (OTFTs) [2–7]. Unlike p-type organic materials, the development of high-performance ambient-stable n-type organic materials has lagged far behind that of p-type organic materials [8]. In the past few years, this situation has been greatly changed due to the increasing attention in this field. Several high-performance n-type organic materials have been developed, and the devices fabricated by vapor deposition methods also exhibit high stability in ambient conditions. Specific progress in performance and molecular design of n-type organic semiconductors in the past 5 years have been reviewed by Liu et al. [9]. However, as far as solution-processable n-channel semiconductors are concerned, it is still challenging to fabricate high-performance ambient-stable n-channel OTFTs.

Excellent n-type organic semiconductors require not only relatively large electron affinity [10–13] but also high electron mobilities [14–17]. The semiconductor materials

---

**Electronic supplementary material** The online version of this article (doi:[10.1007/s00214-010-0841-4](https://doi.org/10.1007/s00214-010-0841-4)) contains supplementary material, which is available to authorized users.

G. Yang · Y. Si · Y. Geng · F. Yu · Q. Wu · Z. Su (✉)  
Institute of Functional Material Chemistry,  
Faculty of Chemistry, Northeast Normal University,  
130024 Changchun, Jilin, People's Republic of China  
e-mail: zmsu@nenu.edu.cn

Y. Si  
College of Resource and Environmental Science,  
Jilin Agricultural University, 130118 Changchun,  
Jilin, People's Republic of China

with relatively large electron affinity permit efficient electron injection into the LUMO of semiconductor molecules and increase thermodynamic stability of devices. The rational design of new organic materials exhibiting nonconventional optoelectronic properties is based on the synthesis of molecules with appropriate geometrical and electronic structures [18, 19]. It is known that quinones act as organic oxidizing reagents in organic synthesis and biological systems. Studies show that nitrogen-rich heteroacenes are promising n-type organic semiconductors [20, 21]. Based on these structural and electronic features, N-heteroquinones (Fig. 1) are synthesized and can function as n-type organic semiconductors in OTFTs with high electron mobility [22]. Here, 5,7,12,14-tetraaza-6,13-penta-cenequinone (**TAPQ**) compound was taken as an example to analyze its structural characters in crystal environment (Fig. 1). **TAPQ** can form close  $\pi$ – $\pi$  stacking with a distance of 3.32 Å and four intermolecular DDAA–AADD (D is hydrogen donor and A is hydrogen acceptor) pattern hydrogen bonds. The  $\pi$ – $\pi$  stacking mainly occurs along *a* axis direction, while the quadruple hydrogen bond interactions along the *bc* plane. Up to now, it is not clear that their carrier transport properties are determined whether by the intermolecular  $\pi$ – $\pi$  interactions or by intermolecular hydrogen bonds. This provides good model compounds for us to study the relationship between them.

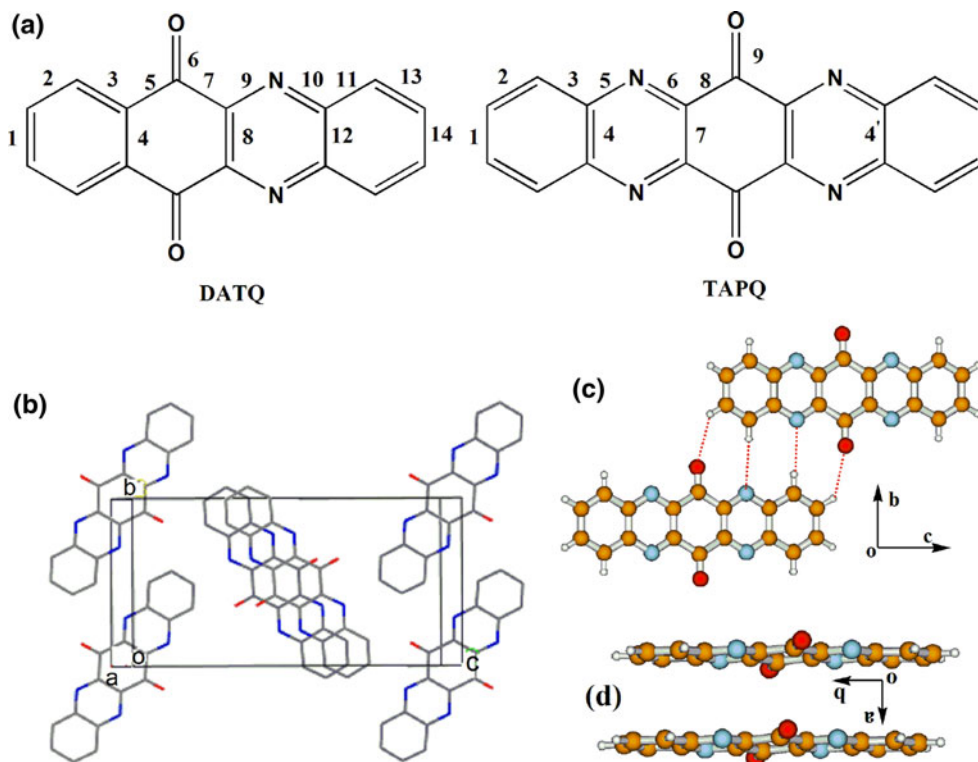
With the development of photoelectric theory and quantum-chemical computational method, it is possible to

explain the experimental phenomenon and design excellent photoelectric materials. For example, Bredas et al. have systematically investigated charge transport in organic semiconductors [14] and energy-transfer processes in  $\pi$ -conjugated oligomers and polymers [23]. Shuai et al. quantitatively calculated the molecular fluorescence quantum efficiency under harmonic approximation by considering the Duschinsky rotation effect [24]. Frenking and Zhang have studied Alq<sub>3</sub> by quantum-chemical analysis, which is very helpful for understanding its chemical bonds and photophysical properties [25]. Our group also investigated the charge transport mechanism and photophysical properties of a series of organic photoelectric materials [26–29]. In this paper, we focus on studying photophysical properties, determining the mechanism of electron or hole transport, exploring the relationships between reorganization energy and bond-length changes upon oxidation or reduction of the two novel N-heteroquinones compounds with the assistance of quantum-chemical calculations.

## 2 Theoretical methodology

The geometry of neutral, cation, and anion states was optimized at the density functional theory level with the B3LYP functional, involving the gradient correction of the exchange functional by Becke [30, 31] and the correction functional by Lee, Yang and Parr, [31] employing a

**Fig. 1** **a** Chemical structures of **DATQ** and **TAPQ**. **b** Crystal structure of **TAPQ**. **c** Crystal structure of **TAPQ** viewed along the *bc* plane, which are formed by intermolecular hydrogen bonding interactions. **d** Crystal structure of **TAPQ** viewed along *a* axis direction, which are formed by strong intermolecular  $\pi$ – $\pi$  interactions



6-31G\* basis set using the Gaussian 03 program suite [32]. No symmetry or internal coordinate constraints were applied during optimization. The electronic absorption spectra were systematically investigated by time-dependent density functional theory (TD-DFT) based on the optimized structures.

The hopping model [33–39] was employed to calculate the carrier mobility in which charge can transfer only between neighboring molecules. In this case, the charge transport mechanism can be described as involving a self-exchange electron transfer from a charged molecule to an adjacent neutral molecule. The rate of charge transfer between neighboring molecules,  $k$ , can be expressed by the standard Marcus equation [40, 41] in terms of the reorganization energy  $\lambda$ , the transfer integral  $t$ , and the temperature  $T$  as

$$k = \frac{4\pi^2}{h} \frac{1}{\sqrt{4\pi\lambda k_B T}} t^2 \exp\left(-\frac{\lambda}{4k_B T}\right) \quad (1)$$

where  $h$  and  $k_B$  are the Planck and Boltzmann constants. To get larger transfer rate, it needs the larger transfer integral and the smaller reorganization energy. The drift mobility of hopping,  $\mu$ , can be evaluated from the Einstein relation

$$\mu = \frac{e}{k_B T} D \quad (2)$$

where  $e$  is the electronic charge and  $D$  is the diffusion coefficient, which is related to the charge-transfer rate  $k$  as summing over all possible hops. The diffusion coefficient can be approximately evaluated as [42–46]

$$D = \frac{1}{2n} \sum_i d_i^2 k_i P_i \quad (3)$$

where  $n$  is equal to 3, which is the dimensionality of space,  $k_i$  is the hopping rate due to the charge carrier to the  $i$ th neighbor,  $d_i$  is the distance to neighbor  $i$ , and  $P_i$  is the relative probability for charge carrier to a particular  $i$ th neighbor

$$P_i = k_i / \sum_i k_i. \quad (4)$$

To study the anisotropy of charge transport, the electronic band-structure calculations were performed with VASP [47–49] using the PBE (Perdew-Burke-Ernzerhof) exchange–correlation functional [50] and a plane-wave basis set. Electron–ion interactions were described using the projector augmented wave (PAW) method [51–53]. The kinetic energy cutoff on the wave function expansion was set to 500 eV. The band-structure calculations were based on the optimized crystal structure, and the cell constants were fixed at the experimental values during optimization, with a Monkhorst–Pack mesh of  $10 \times 4 \times 2$  k-points

### 3 Results and discussion

#### 3.1 Electron spectra

Time-dependent density functional theory (TDDFT) has emerged as the currently most applied method for molecular computations due to its balance between accuracy and efficiency. The electron transition energies, oscillator strengths, and major transition contribution of the studied compounds have been calculated by TDDFT method based on the optimized ground state geometry (Fig. 1) and listed in Table 1. The calculated transition energies agree with the experimental results. This indicates that our adopted method is suitable to the studied compounds. The maximum transitions of 6,11-diaza-5,12-tetracenequinone (**DATQ**) and **TAPQ** are characterized by electron promotion from the HOMO-4 to the LUMO + 1 and the HOMO-5 to the LUMO, respectively. These electronic transitions possess  $\pi \rightarrow \pi^*$  character (Fig. 2). Moreover, the oscillator strength of **TAPQ** is larger than that of **DATQ**, which is also observed in the experimental measurement.

#### 3.2 Reorganization energy

The inner reorganization energy can be computed either from adiabatic potential energy surfaces [36] or from normal mode calculations [54, 55]. The adiabatic potential energy surfaces method combined with B3LYP functional has been widely employed for calculating reorganization energies of the charge transport processes [35, 36, 38, 56, 57]. The calculated reorganization energies based on the adiabatic potential energy surfaces method are given in Table 2. Overall, the electron reorganization energies are much smaller than of hole reorganization energies. Especially, the value  $\lambda_e$  (0.12 eV) of **TAPQ** is smaller than the value  $\lambda_e$  (0.27 eV) of **Alq** which is a typical electron transport material [58]. This indicates that the studied compounds could be a good electron transport material from the standpoint of reorganization energy. Both electron and hole reorganization energies of **TAPQ** are smaller than those of **DATQ**, which can be explained from the analysis of bond-length changes upon oxidation or reduction.

There is a close relationship between charge transport and bond-length changes upon oxidation or reduction. In general, the smaller bond-length changes in these processes

**Table 1** Absorption energies (nm), oscillator strength ( $f$ ), major contribution, and experimental data

Compounds	Experiment	Theory	$f$	Major contribution
<b>DATQ</b>	284	290.5	0.59	HOMO-4 → LUMO + 1
<b>TAPQ</b>	300	307.5	1.08	HOMO-5 → LUMO

**Fig. 2** Molecular orbitals involved into the main absorption transition

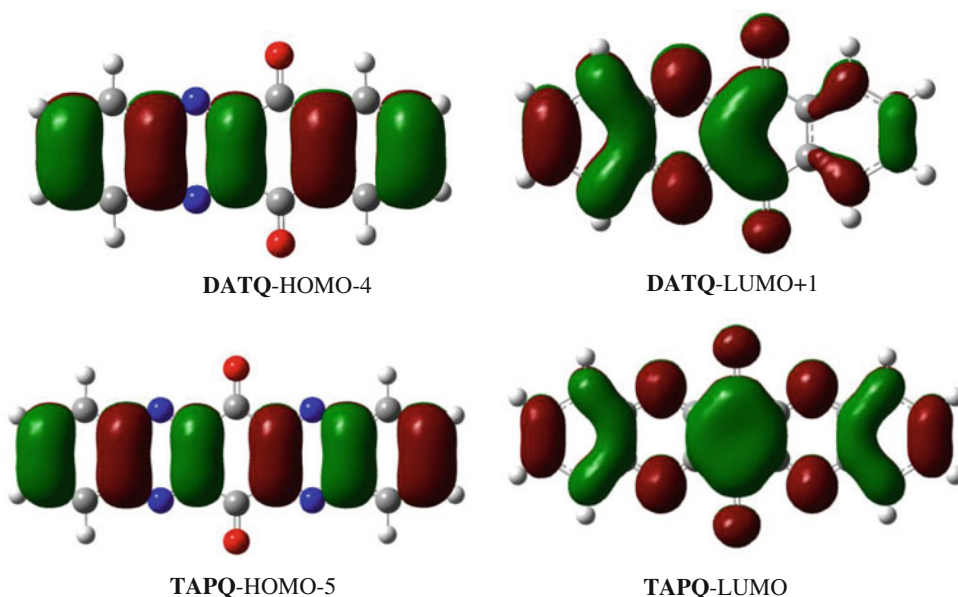


**Table 2** Calculated hole ( $\lambda_h$ ) and electron ( $\lambda_e$ ) reorganization energies (eV) of the studied compounds at B3LYP/6-31G\* level

Compounds	$\lambda_h$	$\lambda_e$
<b>DATQ</b>	0.66	0.32
<b>TAPQ</b>	0.37	0.12

would exhibit the smaller reorganization energy, which would lead to the easier charge transport. The geometry modifications occurring upon oxidation and reduction of the studied compounds are listed in Table 3. The bond-length changes of **DATQ** in both oxidation and reduction process are larger than those of **TAPQ**. Therefore, it is not surprising that the reorganization energies of **DATQ** were estimated to be larger than those of **TAPQ**. Here, the reduction process was taken as an example. The largest bond-length changes upon reduction of **TAPQ** are bonds 4 and 4'. While the largest bond-length changes upon reduction of **DATQ** locate at quinone part. The **TAPQ** contains another benzene ring compared with **DATQ** and form a nearly symmetric center around quinone. This means that subtle structural modifications can lead to the obvious different bond-length changes upon reduction and exhibit obvious variation of reorganization energy.

### 3.3 Transfer integral

Currently, three methods are mainly used to calculate transfer integral value, such as site-energy corrected method [59], direct coupling method [60, 61], and simplified energy splitting in dimer (ESD) method [45]. To the studied compounds, the structures of some dimers are asymmetric. To these kinds of structures, ESD method

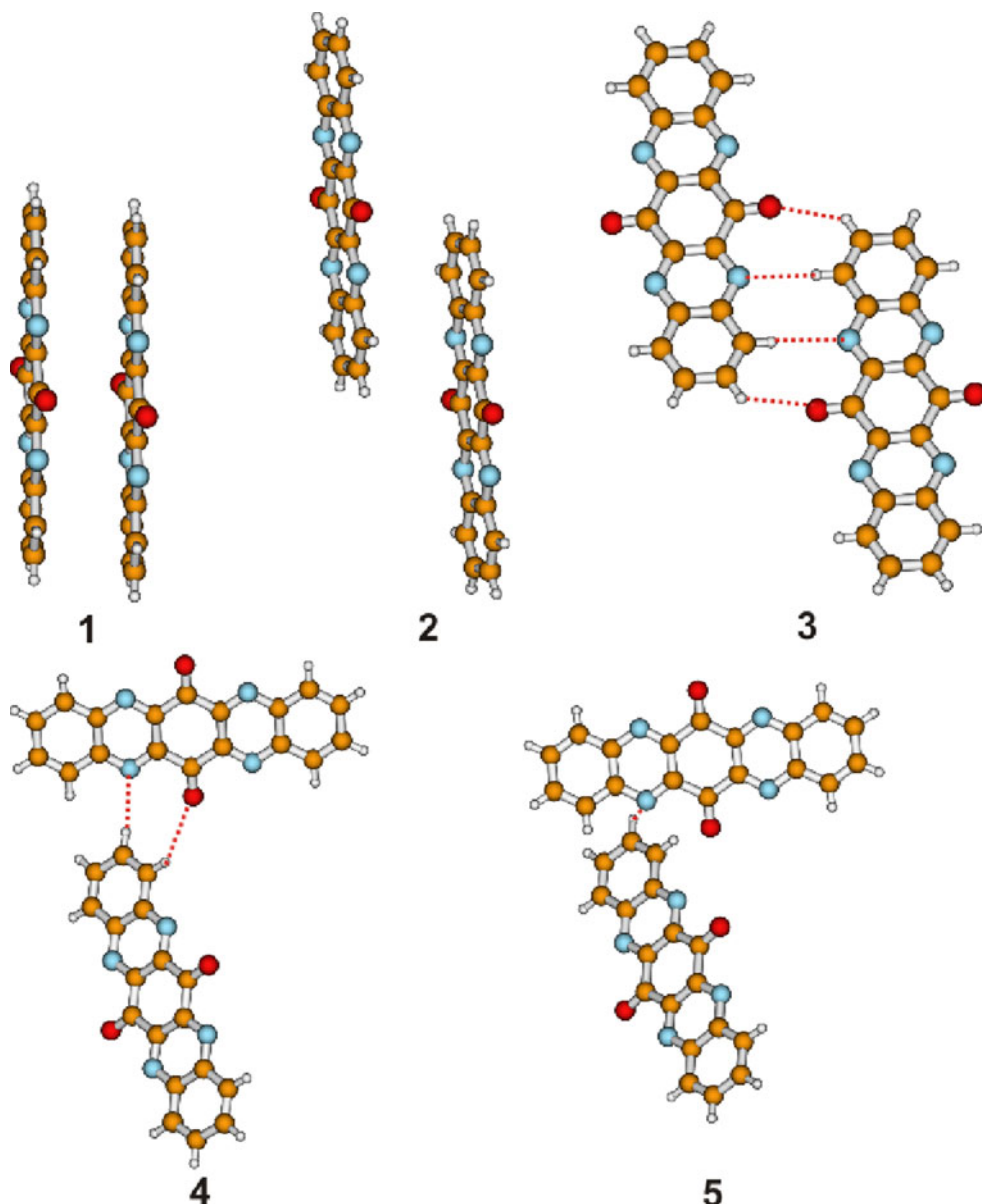
**Table 3** Calculated bond-length changes (in Å) upon oxidation (CBLA, going from the neutral to the cation state) and reduction (ABLA, going from the neutral to the anion state) of the studied compounds

Bonds	<b>DATQ</b>		<b>TAPQ</b>	
	CBLA	ABLA	CBLA	ABLA
1	0.002	-0.015	0.001	0.013
2	-0.003	0.010	-0.002	-0.011
3	0.000	-0.014	0.005	0.007
4	-0.009	-0.016	-0.017	<b>0.023</b>
5	0.017	<b>0.026</b>	0.010	-0.014
6	0.009	<b>-0.032</b>	<b>0.021</b>	-0.008
7	<b>-0.031</b>	<b>0.031</b>	<b>-0.036</b>	0.000
8	<b>-0.036</b>	<b>-0.032</b>	-0.014	0.011
9	<b>0.034</b>	-0.015	0.012	-0.012
10	0.019	0.010	-	-
11	<b>-0.030</b>	-0.004	-	-
12	0.008	-0.007	-	-
13	-0.003	0.003	-	-
14	0.002	-0.006	-	-

Large variations of the CBLA and ABLA values are given in bold

could overestimate the transfer integral value. Thus, the site-energy corrected method and direct coupling method are used to calculate the transfer integral at PW91PW91/6-31G\*\* level [46, 62, 63]. To be simple, **TAPQ** was taken as an example to investigate the influence of hydrogen bonds and  $\pi$ - $\pi$  interactions on transfer integral. All possible charge hopping pathways are shown in Fig. 3. The calculated transfer integral values for both hole and electron are given in Table 4. From Table 4 and Fig. 3, we can draw the following conclusions: (1) The results obtained

**Fig. 3** All charge hopping pathways for the studied compound **TAPQ**



from the site-energy corrected method and direct coupling method are almost the same. (2) The pathways 1 and 2 contain strong intermolecular  $\pi-\pi$  interactions and exhibit large electronic transfer integral value, which means that these pathways containing the intermolecular  $\pi-\pi$  interactions favor the electron transport. Compared with the pathways 1 and 2, electronic transfer integral value increases with enhancement of intermolecular overlap. The pathways 3, 4, and 5 contain intermolecular hydrogen bonding interactions and have large hole transfer integral value, which indicates that these pathways containing the intermolecular hydrogen bonds favor the whole transport. The hydrogen bonding number of the pathways of 3, 4, and 5 is 4, 2, and 1, respectively. The value of hole transfer integral increases with increasing the number of hydrogen bonds. This means that hole transfer integral can be

efficiently tuned through controlling the number of hydrogen bonds. (3) The rate of charge transfer between neighboring is proportional to the square of transfer integral. The electronic transfer integral values obtained from the intermolecular  $\pi-\pi$  packing are much larger than those of hydrogen bonding dimers. Thus, the electron mobility is mainly determined by the intermolecular  $\pi-\pi$  packing. The hole mobility is mainly determined by the hydrogen bonding dimer. The same methods are used to **DATQ** compound. All possible charge hopping pathways and their transfer integral values of **DATQ** are given in Figure S1 and Table S1 available as supplementary material. The results of **DATQ** are similar to those of **TAPQ**. Based on the above discussion, intermolecular electronic couplings are very sensitive to the relative positions of the molecules and the number of intermolecular hydrogen bonds.

**Table 4** The calculated transfer integral value (meV) for both hole and electron of **TAPQ** compound based on direct coupling method and site-energy corrected method

Pathway	Direct coupling method		Site-energy corrected method	
	$t_h$	$t_e$	$t_h$	$t_e$
1	−1.19	59.65	2.78	63.62
2	0.23	−13.95	2.21	2.17
3	46.37	1.30	29.81	2.14
4	−2.32	−1.32	1.93	2.12
5	0.38	2.82	0.29	5.46

**Table 5** The calculated carrier mobilities ( $\text{cm}^2/\text{Vs}$ ) for both hole ( $\mu_h$ ) and electron ( $\mu_e$ ) based on direct coupling method and site-energy corrected method

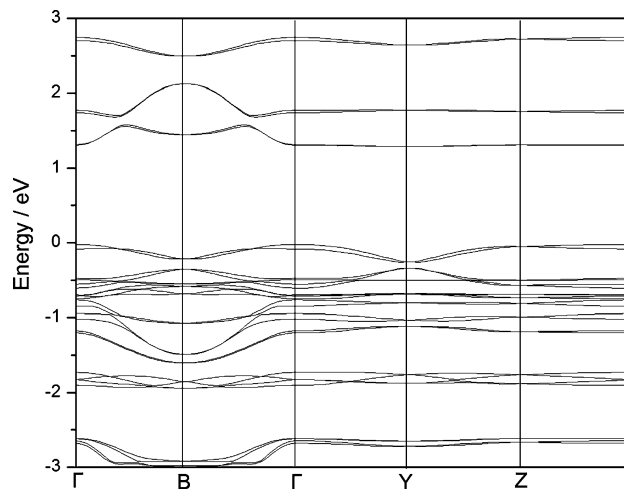
Compound	Direct coupling method		Site-energy corrected method		Experiment
	$\mu_h$	$\mu_e$	$\mu_h$	$\mu_e$	
<b>TAPQ</b>	0.107	0.541	0.043	0.618	0.12
<b>DATQ</b>	0.011	0.016	0.005	0.026	

### 3.4 Carrier mobility

Based on the calculated results of reorganization energy and transfer integral, the carrier mobilities for both hole and electron are calculated using the Eq. 2 and given in Table 5. On the whole, the electron mobilities are larger than the hole mobilities for both **DATQ** and **TAPQ**, which is in agreement with the experimental predication. Furthermore, the two methods give the similar results, and the electron mobility of **TAPQ** is close to the experimentally measured values. This means that our adopted methods are suitable to the studied compounds.

### 3.5 Band structure

Studies of the anisotropy of charge transport in single crystals show that the efficiency of transport is intimately related to the relative positions of the interacting molecules, and hence to crystal packing [14]. To further validate above calculated results and discuss the influence of the anisotropy on the charge transport, the electronic band structure along high-symmetry directions of **TAPQ** is shown in Fig. 4. Due to the two translationally inequivalent molecules present in the unit cell, both occupied and unoccupied bands consist of two sub-bands. In general, there is a close relationship between bandwidth and charge transport. The larger bandwidth is, the larger carrier mobility is. The largest dispersion for conduction band is observed along the symmetry line  $\Gamma \rightarrow \text{B}$  corresponding to

**Fig. 4** Calculated band structure of **TAPQ** crystal. The high-symmetry points are  $\Gamma(0,0,0)$ ,  $\text{B}(0.5,0,0)$ ,  $\text{Y}(0,0.5,0)$ ,  $\text{Z}(0,0,0.5)$ 

the  $a$  axis in real space, which mainly results from the intermolecular  $\pi-\pi$  packing (Fig. 1). However, the largest dispersion for valence band is observed along the symmetry line between  $\text{Y} \rightarrow \Gamma$  and  $\text{Y} \rightarrow \text{Z}$  corresponding to the  $bc$  plane in real space, which results from the intermolecular hydrogen bonds (Fig. 1). This means that intermolecular  $\pi-\pi$  packing are responsible for electron transport and intermolecular hydrogen bonding interactions are responsible for hole transport. Moreover, the bandwidth of conduction band is larger than that of valence band. From the band-structure point of view, the electron in conduction band could move much easier than the holes in valence band, which is agreement with the results of hopping model and experimental measurement.

## 4 Conclusions

N-heteroquinones can function as n-type organic semiconductors in OTFTs with high electron mobility. There are two main kinds of intermolecular interaction forces of the studied compounds in the crystal, which result from intermolecular  $\pi-\pi$  and hydrogen bonds interactions, respectively. N-heteroquinones were taken as model to study the relationships between charge transports and the intermolecular  $\pi-\pi$  interactions or intermolecular hydrogen bonding interactions. The results of hopping model show that the electron transport properties of the studied compounds are mainly determined by pathways containing intermolecular  $\pi-\pi$  interactions, and hole transport properties are mainly determined by pathways containing with intermolecular hydrogen bonds. Electronic transfer integral value increases with enhancement of intermolecular overlap corresponding to the overlap extent of  $\pi-\pi$  packing. Whereas hole transfer integral value decreases with

decreasing the number of hydrogen bonds. This means that charge transport properties can be efficiently tuned by controlling the relative positions of the molecules and the number of hydrogen bonds. The analysis of band structure shows that the electron in conduction band could move much easier than the holes in valence band, which is agreement with the results of hopping model and experimental measurement.

**Acknowledgments** The authors gratefully acknowledge the financial support from the National Natural Science Foundation of China (Project No. 20903020; 20703008), Chang Jiang Scholars Program (2006), Program for Changjiang Scholars and Innovative Research Team in University (IRT0714), National Basic Research Program of China (973 Program—2009CB623605), the Science and Technology Development Project Foundation of Jilin Province (20090146), the Training Fund of NENU's Scientific Innovation Project (NENU-STC08005 and -STC08012), The Project-sponsored by SRF for ROCS, SEM and Open Project Program of State Key Laboratory of Supramolecular Structure and Materials, Jilin University. And we also thank Patrik Callis (MSU) for supplying the Bozesuite program. Science Foundation for Young Teachers of Jilin Agricultural University.

## References

- Yoshiro Y (2009) *Sci Technol Adv Mater* 10:024313
- Newman CR, Frisbie CD, da Silva Filho DA, Bredas JL, Ewbank PC, Mann KR (2004) *Chem Mater* 16:4436–4451
- Zaumseil J, Sirringhaus H (2007) *Chem Rev* 107:1296–1323
- Yamashita Y (2009) *Chem Lett* 38:870–875
- Allard S, Forster M, Souharce B, Thiem H, Scherf U (2008) *Angew Chem Int Ed* 47:4070–4098
- Mayer AC, Scully SR, Hardin BE, Rowell MW, McGehee MD (2007) *Mater Today* 10:28–33
- Anthony JE (2006) *Chem Rev* 106:5028–5048
- Murphy AR, Fréchet JMJ (2007) *Chem Rev* 107:1066–1096
- Wen Y, Liu Y (2010) *Adv Mater* 22:1331–1345
- de Leeuw DM, Simenon MMJ, Brown AR, Einerhand REF (1997) *Synth Met* 87:53–59
- Tang ML, Reichardt AD, Wei P, Bao Z (2009) *J Am Chem Soc* 131:5264–5273
- Usta H, Risko C, Wang Z, Huang H, Deliomeroglu MK, Zhukhovitskiy A, Facchetti A, Marks TJ (2009) *J Am Chem Soc* 131:5586–5608
- Jones BA, Facchetti A, Wasielewski MR, Marks TJ (2007) *J Am Chem Soc* 129:15259–15278
- Coropceanu V, Cornil J, da Silva Filho DA, Olivier Y, Silbey R, Brédas JL (2007) *Chem Rev* 107:926–952
- Brédas JL, Calbert JP, da Silva Filho DA, Cornil J (2002) *Proc Natl Acad Sci USA* 99:5804–5809
- Ando S, Murakami R, Nishida JI, Tada H, Inoue Y, Tokito S, Yamashita Y (2005) *J Am Chem Soc* 127:14996–14997
- Bao Z, Lovinger AJ, Dodabalapur A (1996) *Appl Phys Lett* 69:3066–3068
- Nalwa H (1997) *Handbook of organic conductive molecules and polymers*, vol 1 C4. Wiley, New York
- Balzani V, Venturi M, Credi A (2003) *Molecular devices and machines: a journey into the nano world*; Vch Verlagsgesellschaft Mbh
- Winkler M, Houk KN (2007) *J Am Chem Soc* 129:1805–1815
- Miao S, Appleton AL, Berger N, Barlow S, Marder SR, Hardcastle KI, Bunz UHF (2009) *Chem Eur J* 15:4990–4993
- Tang Q, Liang Z, Liu J, Xu J, Miao Q (2010) *Chem Comm* 46:2977–2979
- Bredas JL, Beljonne D, Coropceanu V, Cornil J (2004) *Chem Rev* 104:4971–5004
- Peng Q, Yi Y, Shuai Z, Shao J (2007) *J Am Chem Soc* 129:9333–9339
- Zhang J, Frenking G (2004) *J Phys Chem A* 108:10296–10301
- Yang GC, Su T, Shi SQ, Su ZM, Zhang HY, Wang Y (2007) *J Phys Chem A* 111:2739–2744
- Yang GC, Liao Y, Su ZM, Zhang HY, Wang Y (2006) *J Phys Chem A* 110:8758–8762
- Gao HZ, Qin CS, Zhang HY, Wu SX, Su ZM, Wang Y (2008) *J Phys Chem A* 112:9097–9103
- Wu J, Wu SX, Geng Y, Yang GC, Shabbir M, Jin JL, Liao, Su ZM, (2010) *Theor Chem Acc*. doi:[10.1007/s00214-010-00730-x](https://doi.org/10.1007/s00214-010-00730-x)
- Becke AD (1993) *J Che Phys* 98:1372–1377
- Lee C, Yang W, Parr RG (1998) *Phys Re B* 37:785
- Frisch MJ, Trucks GW, Schlegel HB, Scuseria GE, Robb MA, Cheeseman JR, Montgomery JA Jr, Vreven T, Kudin KN, Burant JC, Millam JM, Iyengar SS, Tomasi J, Barone V, Mennucci B, Cossi M, Scalmani G, Rega N, Petersson GA, Nakatsuji H, Hada M, Ehara M, Toyota K, Fukuda R, Hasegawa J, Ishida M, Nakajima T, Honda Y, Kitao O, Nakai H, Klene M, Li X, Knox JE, Hratchian HP, Cross JB, Adamo C, Jaramillo J, Gomperts R, Stratmann RE, Yazyev O, Austin AJ, Cammi R, Pomelli C, Ochterski JW, Ayala PY, Morokuma K, Voth GA, Salvador P, Dannenberg JJ, Zakrzewski VG, Dapprich S, Daniels AD, Strain MC, Farkas O, Malick DK, Rabuck AD, Raghavachari K, Foresman JB, Ortiz JV, Cui Q, Baboul AG, Clifford S, Cioslowski J, Stefanov BB, Liu G, Liashenko A, Piskorz P, Komaromi I, Martin RL, Fox DJ, Keith T, Al-Laham MA, Peng CY, Nanayakkara A, Challacombe M, Gill PMW, Johnson B, Chen W, Wong MW, Gonzalez C, Pople JA (2003) *GAUSSIAN 03*, (Revision C.02). Gaussian, Inc., Pittsburgh
- Nelsen SF, Triebel DA, Ismagilov RF, Teki Y (2001) *J Am Chem Soc* 123:5684–5694
- Nelsen SF, Blomgren F (2001) *J Org Chem* 66:6551–6559
- Sakanoue K, Motoda M, Sugimoto M, Sakaki S (1999) *J Phys Chem A* 103:5551–5556
- Malagoli M, Brédas JL (2000) *Chem Phys Lett* 327:13–17
- Li XY, Tong J, He FC (2000) *Chem Phys* 260:283–294
- Lin BC, Cheng CP, Lao ZP (2003) *J Phys Chem A* 107:5241–5251
- Marcus RA (1985) *Biochim Biophys Acta* 811:265
- Marcus RA (1993) *Rev Mod Phys* 65:599
- Balzani V, Juris A, Venturi M, Campagna S, Serroni S (1996) *Chem Rev* 96:759–834
- Deng WQ, Goddard WA (2004) *J Phys Chem B* 108:8614–8621
- Song Y, Di CA, Yang X, Li S, Xu W, Liu Y, Yang L, Shuai Z, Zhang D, Zhu D (2006) *J Am Chem Soc* 128:15940–15941
- Schein LB, McGhie AR (1979) *Phys Rev B* 20:1631
- Yang XD, Li Q, Shuai ZG (2007) *Nanotechnology* 18:424029
- Yang XD, Wang L, Wang C, Long W, Shuai Z (2008) *Chem Mater* 20:3205–3211
- Kresse G, Furthmüller J (1996) *Comput Mater Sci* 6:15–50
- Kresse G, Hafner J (1993) *Phys Rev B* 47:558
- Kresse G, Hafner J (1994) *Phys Rev B* 49:14251
- Perdew JP, Burke K, Ernzerhof M (1996) *Phys Rev Lett* 77:3865
- Blöchl PE (1994) *Phys Rev B* 50:17953
- Kresse G, Joubert D (1999) *Phys Rev B* 59:1758
- Monkhorst HJ, Pack JD (1976) *Phys Rev B* 13:5188
- Malagoli M, Coropceanu V, Filho DA, Bredas JL (2004) *J Chem Phys* 120:7490–7496

55. da Silva Filho DA, Coropceanu V, Fichou D, Gruhn NE, Bill TG, Gierschner J, Cornil J, Brédas JL (2007) *Philos Trans R Soc London A* 365:1435–1452
56. Gruhn NE, da Silva Filho DA, Bill TG, Malagoli M, Coropceanu V, Kahn A, Brédas JL (2002) *J Am Chem Soc* 124:7918–7919
57. Coropceanu V, Malagoli M, da Silva Filho DA, Gruhn NE, Bill TG, Brédas JL (2002) *Phys Rev Lett* 89:275503
58. Lin BC, Cheng CP, You ZQ, Hsu CP (2004) *J Am Chem Soc* 127:66–67
59. Valeev EF, Coropceanu V, da Silva Filho DA, Salman S, Brédas JL (2006) *J Am Chem Soc* 128:9882–9886
60. Hutchison GR, Ratner MA, Marks TJ (2005) *J Am Chem Soc* 127:16866–16881
61. Troisi A, Orlandi G (2001) *Chem Phys Lett* 344:509–518
62. Irfan A, Zhang JP, Chang YF (2009) *Chem Phys Lett* 483:143–146
63. Li L, Tang Q, Li H, Yang X, Hu W, Song Y, Shuai Z, Xu W, Liu Y, Zhu D (2007) *Adv Mater* 19:2613–2617